Composites: Part A 87 (2016) 282–289

Contents lists available at ScienceDirect

Composites: Part A

journal homepage: www.elsevier.com/locate/compositesa

An analytical model for B-stage joining and co-curing of carbon fibre epoxy composites

J. Studer [b], C. Dransfeld [b], K. Masania [a,b,*]

[a] Complex Materials Group, Department of Materials, ETH Zürich, Vladimir-Prelog Weg 5, 8093 Zurich, Switzerland
[b] Institute of Polymer Engineering, FHNW University of Applied Sciences and Arts Northwestern Switzerland, Klosterzelgstrasse 2, 5210 Windisch, Switzerland

ARTICLE INFO

Article history:
Received 19 January 2016
Received in revised form 4 May 2016
Accepted 7 May 2016
Available online 9 May 2016

Keywords:
A. Thermosetting resin
B. Cure behaviour
C. Process simulation
E. Assembly

ABSTRACT

The objective of this paper was to develop cure kinetic models to describe the B-stage curing and co-curing assembly of carbon fibre reinforced thermosetting polymer (CFRP) composites. Starting from the analytical model, temperature cycles and experimental procedures are developed to join a B-stage CFRP part to a reinforcing B-stage CFRP patch for local reinforcement. Our results show that by using the analytical model, one may precisely describe the cure reaction and join the composites without any additional adhesive. The co-cured composites were successfully manufactured with stable fibre volume fractions and glass transition temperatures between the two sub-components. Additionally, merits of the process, such as modifying reinforcing areas locally, or formation of net shape detail are discussed.

1. Introduction

The aviation industry is employing evermore carbon fibre reinforced thermosetting polymer (CFRP) structures in order to minimise weight, and hence emissions during flight. However, much of the efficiency that can be gained by using such materials is lost due to inefficient joining procedures and strict certification standards that prevent adhesive joining of primary structures in civil aviation [1]. A solution may be to partially cure two sub-assemblies, combine them and complete the cure cycle for both; termed co-curing for this study. By better understanding the resin kinetics and developing procedures that allow co-curing, cost effective manufacturing steps may be utilised e.g. staged curing [2,3], to effectively cure and locally reinforce structural composite materials with thermoset (epoxy) matrices.

A melding approach has been reported by Griffiths and Corbett [4,5], whereby a small region of the part remains in a B-stage cured state by keeping said region at a lower temperature than the structure, thus at a low degree of cure, α, in the joining region whilst the rest of the part is fully cured. However, significant machine infrastructure would be required to produce such structures, also described by Bond [6], which may be expensive to implement. Co-cured joints also provide higher fracture toughness [7] and joint strength [8] than co-bonded joints due to mechanical intermingling and covalent bonding of the resins at the interface [9], adding value to the approach. Further, their mechanical properties have been modelled as they evolve during the curing process [10], hence important knowledge of how properties evolve with cure are available. Application of the co-curing approach for bigger structures requires dedicated tooling, in order to control temperature and resin flow locally [11,12]. Moreover, by producing the structure and local reinforcements separately, valuable freedom is achieved to enhance properties locally, e.g. in the amount of toughener [13,14] that may be introduced, or the reinforcing area or ply thickness that is chosen [15].

Cure kinetic modelling of thermoset resins is widely used and has been described in [16–24]. Most works focus on wide temperature ranges, model optimisation for a wide range of degree of cure or address approaches to control heat exotherm in modern formulations [25]. However, during the curing of a composite structure, the temperature varies in a few degrees around an optimum temperature. Until now such models have had limited possibility for B-stage curing and co-curing to be employed in a robust manner. Moosburger et al. [26] have demonstrated that partial cure of a tetrafunctional epoxy resin maintains its remaining chemical reactivity, the network formation is however slightly influenced by the cure history, hence careful study is needed to fully develop the epoxy network with an interrupted curing process. To our knowledge, no such study has addressed the use of cure modelling to join structures without adhesives.

This work demonstrates an approach for using the developed kinetic model to describe the B-stage curing and co-curing assem-

* Corresponding author at: Complex Materials Group, Department of Materials, ETH Zürich, Vladimir-Prelog Weg 5, 8093 Zurich, Switzerland.
E-mail address: kunal.masania@mat.ethz.ch (K. Masania).

http://dx.doi.org/10.1016/j.compositesa.2016.05.009
1359-835X/

bly of local reinforcement. Starting from the model, temperature cycles are developed to join a B-staged CFRP patch to a B-staged CFRP part by co-curing whilst carefully monitoring the evolution of degree of cure and glass transition temperature, T_g. The example shown in this work explains a methodology to locally reinforce a bearing joint for enhanced bearing load, see Fig. 1.

A simple methodology is presented, that allows the combination of multiple manufacturing processes. The results presented may be directly employed to co-cure structures with various thermosetting resins in an efficient and cost effective manner.

2. Materials

The resin used is "HexFlow RTM6", Hexcel, UK. It is a monocomponent resin system consisting of a tetrafunctional epoxy component, tetraglycidyl 4-4′ diaminodiphenylmethane (TGDDM, Araldite MY 721), and two amine hardeners: 4,4′-Methylene-bis(2,6-diethylanaline) (MDEA, Lonzacure) and 4,4′-Methylene-bis(2,6-diisopropylaniline) (MMIPA, Lonzacure). The resin is a hot curing system with a high T_g developed for infusion and RTM processes.

CFRP parts were manufactured by a RTM process from a biaxial stitched non-crimp fabric, "ECS6090-Series HTS 40", Saertex GmBH & Co., Germany, with an area weight of 256 g/m^2. Quasi-isotropic parts were made from 16 plies: $2[0/90, +45/-45, 90/0, -45/+45]_s$ to produce $150 \times 90 \times 3.8$ mm plates.

The reinforcing CFRP patches were manufactured from a thin ply material, 20 mm tape, 80 g/m^2 high tensile strength carbon fibre "TeXtreme Spread Tow", Oxeon AB, Sweden. Quasi-isotropic, 2 mm thick, 80 mm diameter, ∅ 10 mm hole patches were made from 24 layers of the spread tow with the layup $3[45, 90, -45, 0]_s$.

A nylon peel ply (Econostich, Aero Consultants AG, Nänikon, Switzerland) was used to prepare surfaces for co-curing.

3. Experimental

The differential scanning calorimetry (DSC) measurements were made using a "Q1000 Differential Scanning Calorimeter", TA Instruments, Delaware, USA. Typically, 2–3 mg samples and Nitrogen (flow rate of 50 ml/min) was used as a purge gas. The heat of reaction, ΔH, was calculated with a linear baseline for the integration and T_g was measured as the point of inflexion in the heat flow versus temperature curve.

3.1. Resin cure kinetics

Isothermal and dynamic DSC measurements of the uncured resin were made as reference data for the analytical modelling.

The isothermal heat of reaction, ΔH_{iso}, was evaluated from the isothermal measurements as

$$\Delta H_{iso} = \int_0^{t_c} \frac{dH}{dt} \tag{1}$$

where $\frac{dH}{dt}$ is the heat flux and t_c is the curing time. A second dynamic measurement at 10 °C/min from 0 °C to 300 °C was made to obtain the residual heat of reaction, ΔH_{res}, of the same sample. By adding the two values, the total heat of reaction, ΔH_{tot}, was calculated.

$$\Delta H_{tot} = \Delta H_{iso} + \Delta H_{res} \tag{2}$$

The dynamic heat of reaction, ΔH_{rate}, was obtained from the integration of the dynamic measurements, as

$$\Delta H_{rate} = \int_0^{t_c} \frac{dH}{dt} \tag{3}$$

Isothermal measurements were conducted at 120-, 140-, 160-, and 180 °C, and two measurements per temperature were made. Dynamic measurements were made with a constant heating rate of 1-, 2.5-, 5-, and 10 °C/min until the cross linking reaction was complete. The ultimate heat of reaction, ΔH_{ult}, corresponding to a degree of cure, α, of 1 was determined from the dynamic DSC measurements at 2.5 °C/min. The evaluation of α with time or heating rate was then calculated as follows:

$$\alpha = \frac{\int_0^t \frac{dH}{dt}}{\Delta H_{ult}} \tag{4}$$

3.2. B-stage degree of cure

A series of temperature modulated DSC (MDSC) measurements were used to measure α and T_g of the partially cured resin. This was especially useful as the residual reaction immediately followed the glass transition. The temperature was modulated with ±0.3 °C every 15 s with a heating rate of 10 °C/min up to 300 °C.

The exothermic peak in ΔH_{res} of the nonreversible heat flow was then linear integrated. With a known value of ΔH_{ult} (as measured using the dynamic DSC measurements) α was calculated as

$$\alpha = 1 - \frac{\Delta H_{res}}{\Delta H_{ult}} \tag{5}$$

The value of T_g of the partially cured samples was measured by taking the temperature at the point of inflexion in the reversible heat flow versus temperature curve using pure resin samples or resin samples taken from the produced composites after B-stage curing.

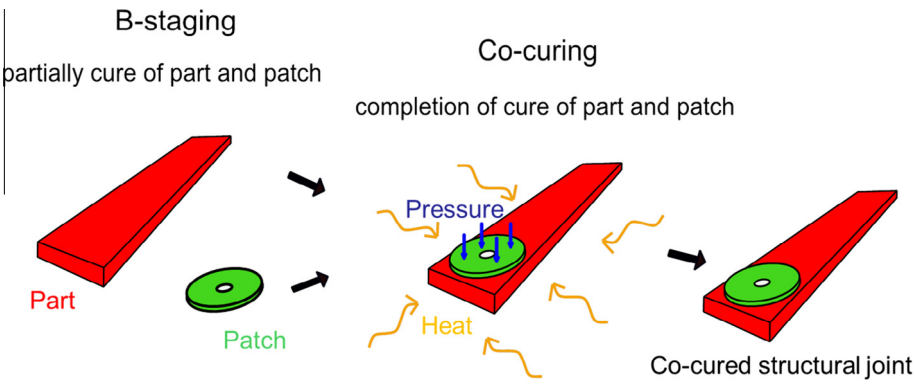

Fig. 1. Shows the concept of patch reinforcement of a structural part via co-curing of B-stage cured components. (For interpretation of the references to colour in this figure legend, the reader is referred to the web version of this article.)

3.3. B-stage curing of the CFRP part and patch

The resin was heated to 80 °C for one hour, then transferred to a plate heated vacuum oven, and degassed to 20 kPa for five minutes, and then to circa 0.8 kPa vacuum pressure for a further 25 min (total preconditioning of 1.5 h at 80 °C). Typically, the degree of cure was found to have evolved a little and was found to vary from batch to batch of resin. This was taken into account to provide a stable baseline from which to predict the degree of cure.

The CFRP parts were cured at 400 kPa for varying times at 160 °C, depending on the desired value of α. Completely cured parts were cured at 180 °C for 90 minutes in the RTM tool, in accordance to [27]. The tool was heated and cooled using a "LaboPress P200T", Vogt, Germany. The B-stage cured CFRP parts were cured at 160 °C in the RTM tool and then cooled rapidly to stop the curing reaction at a desired value of α. It is noted that a desired B-stage α can also be achieved with a slow cooling of the RTM tool.

The CFRP patches were partially cured using a compression RTM at 2 MPa for varying times at 160 °C depending on the desired value of α. The developed model was used to obtain α for the CFRP part and patch samples using direct temperature measurement from the tool. Two temperature sensors: type "SW 154X", Sawi, Switzerland, were integrated 1 mm from the surface of the CFRP patch or CFRP part within their respective tools. The sensor signals were processed in LabView to produce a real time output of α using the predictive models, where a typical example of the tool temperature and calculation of degree of cure is shown in Fig. 2. The MDSC measurements were used to verify the value of α that was given by the model and to obtain T_g of the partially cured, pure resin samples. These samples were taken from excess resin regions at the edge of the part or the patch, ensuring that the sample was free of fibres. To prepare the surface for subsequent co-curing, a nylon peel ply (Econostich), was introduced during B-stage curing and removed before co-curing.

3.4. Co-curing of the CFRP part and patch

The CFRP patch and CFRP part were prepared by first removing peel plies to provide a clean surface for adhesion. Next, the two components were assembled in a silicone ring sealed compression jig. This jig served the purpose of (i) encasing the CFRP patch to a net shape with hole, and (ii) applying a consolidation pressure to provide intimate contact of the CFRP part to the patch. A series of cup springs in the jig were used to set the applied consolidation pressure, and maintain this pressure (2 MPa) as resin from the CFRP patch flowed and the thickness of patch reduced. An H6 Ø10 mm precision bolt was used to provide the tolerance of the hole in the assembled structure, as well as to assemble the jig through the CFRP part. The jig weight was minimised during design, to reduce creep stress by weight on the self-supporting part during the co-curing process.

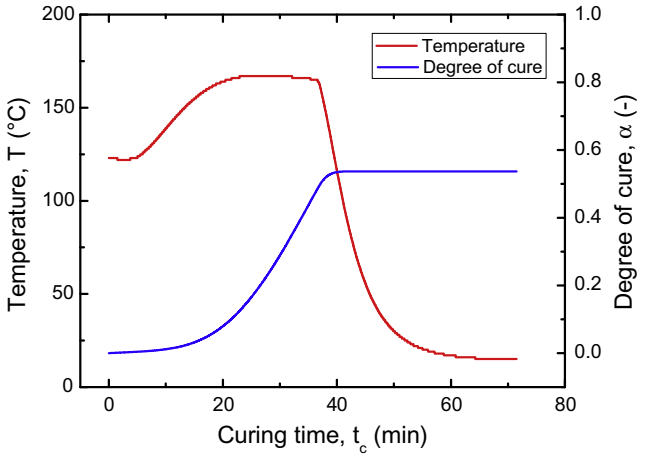

Fig. 2. Curing temperature, T, and degree of cure, α, monitoring for a RTM part using the global kinetic model. (For interpretation of the references to colour in this figure legend, the reader is referred to the web version of this article.)

Double lap bearing test were conducted on the co-cured joint in accordance to procedure B of ASTM D5961 [28] with a Ø10 mm bolt, using a constant displacement rate of 2 mm/min. Optical microscopy of the tested co-cured joint were prepared by polishing epoxy resin-embedded samples with a "TegraPol-21", Struers GmbH, Switzerland, using progressively finer grades of emery paper from 240 to 2400 grit. Polishing was performed up to 0.25 μm diamond polishing solution. A "VKX-200", Keyence, Germany, 3D laser scanning microscope was used to obtain the optical cross sectional images.

4. Models and methodology

The curing reaction was characterised using DSC of the pure resin at different temperatures and heating rates [29,30]. With these measurements, the kinetics of the curing reaction of the resin were investigated. The isothermal and constant heating rate measurements were used to fit a kinetic model to study α and T_g as a function of curing time, t_c, and curing temperature, T_c. Existing modelling approaches were studied [16–24] and modified to appropriately describe the cure reaction using the experimental parameters and the fewest mechanistic assumptions. An assessment of these results led to using the DiBenedetto model [18] to describe T_g and a modified Ruiz [24] model to describe the evolution of cure as explained in the following chapter.

Possible cure cycles for the CFRP part and the CFRP patch were defined to fulfil prerequisites for the part to allow a free standing post cure ($T_g > T_c$) and the resin in the patch to flow ($T_g < T_c$) during co-curing in an oven. The tool temperature close to the surface of the composite part was monitored during cure and used as input temperature for the cure kinetic model. Whether a model developed from small pure resin samples could be used to predict α in a composite RTM process in a simple way was also studied.

4.1. Model for evolution of T_g and resin cure kinetics

To describe the T_g as a function of α, the DiBenedetto model [18] in the form introduced by Pascault and Williams [31] is an accepted approach [32,33] and was adopted in this study.

$$T_g = T_{g0} + \frac{(T_{g\infty} - T_{g0})\lambda\alpha}{1-(1-\lambda)\alpha} \tag{6}$$

where T_{g0} and $T_{g\infty}$ correspond to the T_g of the uncured and fully cured resin, and were measured as −15.5 and 215 °C, respectively. The parameter λ was obtained by a sum of least squares fit with the data shown in Fig. 3, where also the resulting model is shown. The T_g model was used to describe the T_g development during B-stage and co-curing. Prediction for values of α above the gel point (α_{gel} = 0.59 [34]) were of importance, since at these α values, the resin with the CFRP part should be formed into an infinite network. For an adequate fitting of T_g in this range, the value of $T_{g\infty}$ was set as a variable in the DiBenedetto model, with the resulting parameters summarised in Table 3.

A general form of a kinetic model to describe the degree of cure, α, in an epoxy polymer may be written as

$$\frac{d\alpha}{dt} = F(\alpha, T) \tag{7}$$

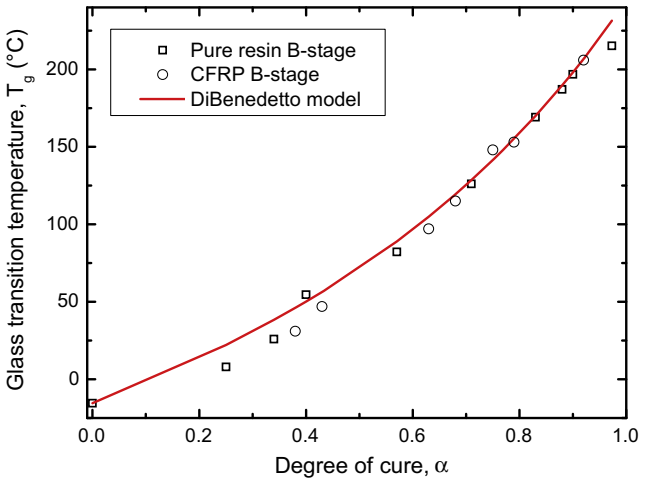

Fig. 3. Correlation of the glass transition temperature, T_g, and the degree of cure, α, using DiBenedetto model based on temperature recorded in cast resin samples. (For interpretation of the references to colour in this figure legend, the reader is referred to the web version of this article.)

where the reaction rate $\frac{d\alpha}{dt}$ is a function of α and T. Amongst the different mechanistic and phenomenological models [16–24], the *n*th order Kamal–Sourour [16] and the Bailleul [20] models shown in (8) are the most common amongst literature [22,23,35–37].

$$\frac{d\alpha}{dt} = K(T)G(\alpha) = k_1 e^{-E_1(T_{ref}/T-1)} \sum_{i=0}^{n} a_1 \alpha^i \tag{8}$$

where k_1 is the frequency factor of the cure reaction, E_1 is the activation energy, T_{ref} is an arbitrarily chosen temperature in the operating range, and $G(\alpha)$ is a polynomial function of order *n*.

To model the cure kinetics precisely, vitrification must be taken into account. During the cure of thermoset resins, the T_g increases while the polymer network grows and vitrification occurs when T_g reaches T_c [38]. In the vitrified state, the reaction changes from chemically controlled to diffusion controlled and the reaction rate decreases significantly. This can be considered in the kinetic model by defining a maximum achievable degree of cure, α_{max}, for each isothermal temperature. The proposed α_{max} model limits the maximum α which can be achieved and is a function of the isothermal curing temperature T_c.

Expanding into the form of a classical kinetic models with an *n*th order term, $(1-\alpha)^n$, and replacing 1 with $\alpha_{max}(T)$ gives

$$\frac{d\alpha}{dt} = k_1 e^{-E_1(T_{ref}/T-1)} \sum_{i=0}^{n} a_1 \alpha^i (1-\alpha)^n \tag{9}$$

combining the Bailleul model (9) with an *n*th order term, so that vitrification can be taken into account gives the Ruiz model [24] shown in (10) as

$$\frac{d\alpha}{dt} = k_1 e^{-E_1(T_{ref}/T-1)} \sum_{i=0}^{n} a_1 \alpha^i (\alpha_{max}(T)-\alpha)^n \tag{10}$$

This model was used for describing the curing reaction.

From the isothermal DSC experiments, α_{max} was obtained experimentally for each curing temperature. By relating α_{max} with T_c instead of relating α with T_g, the DiBenedetto model [18] (6), could be used for predicting α_{max} by solving when $\alpha_{max} = \alpha$ and satisfying $T_g = T_c$; shown in (11):

$$\alpha_{max} = \frac{(T_c - T_{g0})}{(T_{g\infty} - T_{g0})\mu + (1-\mu)(T_c - T_{g0})} \tag{11}$$

where the parameter μ and $T_{g\infty}$ were fit to the obtained α_{max} values using a sum of least squares fit.

The isothermal and the dynamic measurements shown in Fig. 4 were used for the determination of the modelling parameters. A methodology for finding the parameters (K_1, E_1, T_{ref}, and $a_0 - a_i$) of the Bailleul model was described in [20] and was used here. The value of n was optimised using a sum of least squares fit for all experimental measurements.

Two model parameter sets were developed: "global kinetic model" to predict the broader range of degree of cures and "B-stage kinetic model" to predict degree of cure during the B-stage curing. Parameters for both models are summarised in Table 1. The data used as a base for the global kinetic model were isothermal DSC measurements at 120, 140, 160, and 180 °C and dynamic measurements at 1, 2.5, 5 and 10 °C/min.

The global kinetic model, Fig. 5, was found to fit well to the DSC measurements with an R^2 of 0.98, although the vitrification in the low heating rates is not described particularly well. Values of $\alpha = 0.3$ to 0.9 are most interesting when using this model, as B-stage curing and self-supporting co-cure are of importance in this range of degree of cures. The model failed to predict very high conversions of α, above 0.96. The possible reasons are suggested as (i) a single Arrhenius term was used for the overall reaction for simplicity, although it is known that two amine hardener components occur in the resin and (ii) secondary reactions occurring at high α led to the observed inaccuracies. These high conversions were beyond the scope of this work and were not studied further.

To precisely predict α during B-stage curing, more DSC measurements in the range of the B-stage curing temperature (160 °C) were later conducted for optimisation purposes (B-stage kinetic model). The isothermal DSC experiments were conducted for the range 154–166 °C at two degree intervals to provide a precise description of the temperature ranges that the uncured resin would experience in the RTM tool. The parameters of the model were obtained with the same methodology as described previously, except that the isothermal DSC data used as a base for the model changed from 120–180 °C to 154–166 °C. The parameters of this model are shown in Table 3, B-stage kinetic model, resulting in an R^2 of 0.96. With the DiBenedetto model used to describe T_g (α) and the global kinetic model used to describe α (T, t), B-stage curing cycles for the CFRP part and patch could be further studied more precisely.

4.2. B-stage curing cycle of the CFRP part and patch

From a reaction chemistry perspective, α at the intermediate B-stage should be as low as possible for both the CFRP part and the CFRP patch. The lower α, the more unreacted epoxy and amine groups are on the surface, so that covalent bonding between the CFRP part and the CFRP patch is possible. Additionally, the gel point has to be considered, which is reported in [34] as $\alpha_{gel} = 0.59$. The CFRP part ideally, should be stable enough to support its weight during co-curing, avoiding the use of cumbersome co-cure jigs. Thus the T_g of the CFRP part should ideally, remain above T_c during co-curing. Next, the B-stage α of the CFRP patch should be below α_{gel} so that the resin may flow during co-curing and provide the possibility for chemical adhesion to occur. Further, the CFRP patch should also have a high enough T_g to allow handling at room temperature. The curing temperature in the B-stage curing was chosen using the following principal. The B-stage curing is easier to control at lower temperatures, since the curing reaction is slower. However, using a lower cure temperature (100–150 °C) could change the reaction mechanism, which leads to a different network architecture and properties. This is evident by performing a simple measurement of T_g after a low temperature cure cycle. In aerospace composites, aromatic amines are commonly used as hardeners since they lead to the highest T_g where the cure temperature governs reaction rates of primary, or secondary amines with an epoxy

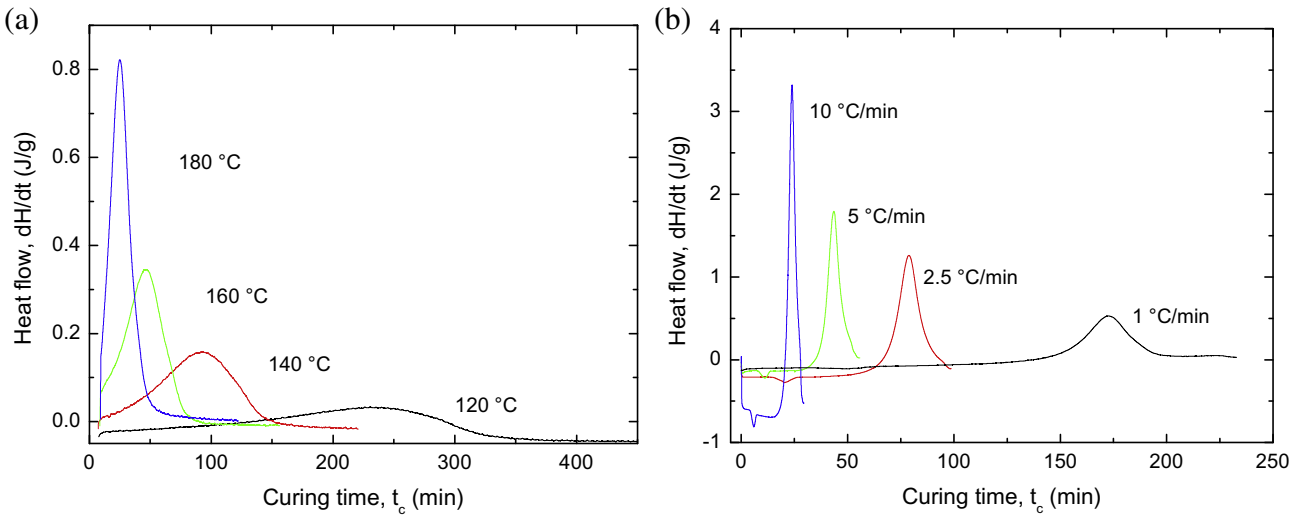

Fig. 4. Shows the heat flow, *dH/dt*, versus curing time, t_c, for (a) isothermal and (b) dynamic measurements of the resin. (For interpretation of the references to colour in this figure legend, the reader is referred to the web version of this article.)

Table 1
Summary of reaction enthalpies from isothermal DSC measurements of the epoxy polymer.

Isothermal curing temperature, T_c (°C)	Reaction enthalpy, ΔH_{iso}(J/g)	Residual reaction enthalpy, ΔH_{res} (J/g)
Global measurement range		
120	392	64
120	393	64
140	407	30
140	418	51
160	435	25
160	432	25
180	443	5
180	450	9
B-stage measurement range		
154	408	48
156	410	47
158	414	48
160	422	48
162	430	38
164	430	40
166	435	37

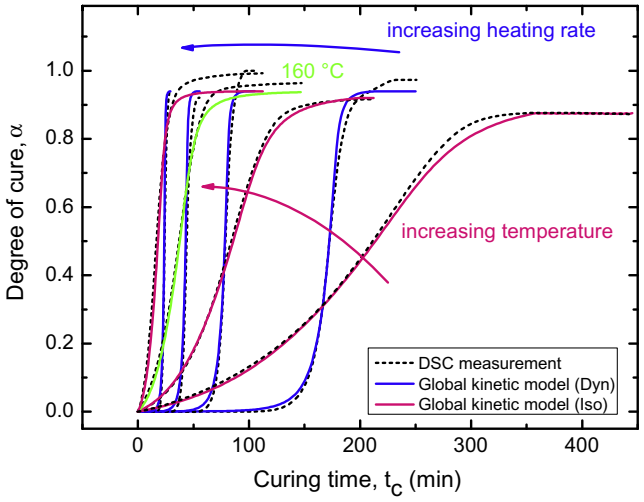

Fig. 5. Shows Comparison of the global kinetic model based on Ruiz model compared to the degree of cure, α, from DSC measurements, where the region of interest is between $\alpha = 0.3$ and 0.9. (For interpretation of the references to colour in this figure legend, the reader is referred to the web version of this article.)

group, or at very high temperatures, self-polymerisation. Therefore, to obtain consistent properties in the part and the patch being joined, both were cured at 160 °C. This temperature is proposed as a possible curing temperature for the RTM6 resin [27], hence easily scalable, and also compliant with documented practises.

The value of α_{patch} was chosen as 0.3, corresponding to T_g just above room temperature, whilst being sufficiently far from the gel point at 0.59 where the resin would stop flowing. The value of α_{part} was selected as 0.75; the lowest possible value so that with a low heating rate, the part may support its own weight during the co-cure process. The cooling and heating rates were selected as per the limitations of our experimental set up. Complete curing cycles that were subsequently used are shown in Fig. 6 for the part and the patch; B-stage followed by assembly and lastly, co-curing.

4.3. Co-curing cycle of the CFRP part and patch

During the co-curing cycle, the T_g of the part defines the upper limit to the heating rate, where T_g is still higher than T_c. This is because if T_g were to dip below T_c, then we would expect deformation of the part structure. Therefore, to shorten the co-curing cycle, first a heating rate of 2.5 °C/min is used until T_c approaches T_g, then the heating rate is reduced to 1 °C/min. When reaching 180 °C, the temperature is held for 60 minutes to ensure full crosslinking in both the part and the patch. With this co-curing cycle, which is identical for the part and the patch, the resin in the patch can flow in a wide range until reaching the gel point, so that all requirements are fulfilled. The isothermal holding times in the B-stage curing and co-curing were chosen to be within the proposed curing cycles of the manufacturer [27], to avoid incomplete or excessive curing.

5. Results

5.1. DSC measurements

The maximum heat of reaction at a cure temperature, ΔH_{iso}, was first determined using isothermal measurements. Fig. 4(a) shows $\frac{dH}{dt}$ versus t_c, where, with increasing cure temperature the reaction rate increases and thus the reaction peak gets narrower

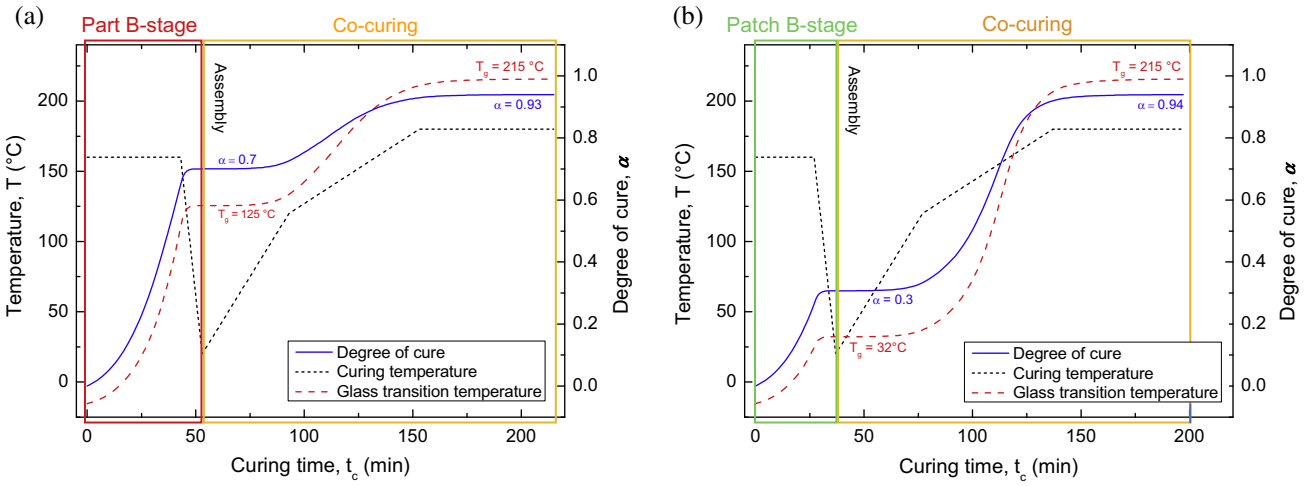

Fig. 6. Curing cycle for the (a) part and (b) patch, showing that the glass transition temperature, T_g, of the part is always above the curing temperature, T_c whereas the T_g of the patch is far below and allows the resin to flow. (For interpretation of the references to colour in this figure legend, the reader is referred to the web version of this article.)

and the reaction time decreases. Integration of these curves gives the heat of reaction, ΔH_{iso}, for each of the cure temperatures. Due to vitrification, the resin cannot fully cure during an isothermal curing process. Vitrification occurs when the T_g of the curing resin reaches the cure temperature, and slows down the cure reaction. Fig. 4(b) shows $\frac{dH}{dt}$ for the dynamic experiments according to t_c. With increasing heating rates, the cure reaction is more exothermic, hence more heat is produced and the time of reaction reduces with increasing heating rate. Table 2 shows the reaction enthalpies for constant heating rate experiments, ΔH_{rate}. As noted in [29], at too high a heating rate, the reaction cannot be completed due to loss of mobility of the polymer molecules after vitrification, whereas at too low a heating rate, not all of the thermal effects occurring may be recorded due to the resolution of the DSC measurements. Similar behaviour was observed in this study, and the maximum ΔH_{rate} was found at 2.5 °C/min. In the second run of the isothermal measurements, a pronounced enthalpy relaxation overlays the start of the residual curing reaction, and complicates the integration of the heat flow curve. Due to these difficulties in evaluating ΔH_{res}, the average value of ΔH_{rate} measured at 2.5 °C/min was used as ultimate heat of reaction, namely 450 J/g. With the modulated dynamic measurements, α and T_g of partially cured pure resin samples and resin samples from the CFRP parts and CFRP patches were determined. The measured degree of cures and glass transition temperatures are shown in Fig. 3 and were used for the T_g model.

5.2. Comparison of the measured and predicted B-stage

For the manufactured CFRP parts and patches, the predicted α obtained from the global kinetic model with the tool temperature as input was then compared to the measured α with MDSC, shown in the triangles in Fig. 7. Although the global kinetic model has a very good fit to the measurement of the pure resin DSC sample at 160 °C, the model fails to predict α of the composite parts at the required accuracy. Two reasons are proposed to explain this: first the recorded curing temperature is measured in the tool close to the cavity and not directly in the resin and therefore tends to overpredict α, and second the curing temperature is not exactly 160 °C but varies with circa ±6 °C. As the aim was to see if it was possible to predict α from the tool temperature the first issue was not studied further as industrial tool sensors may be integrated to the tool surface in direct contact with the resin. The second source of error was addressed by model optimisation in the 160 ± 6 °C temperature range. The parameter identification for the kinetic model was optimised for the temperature range of 154–166 °C. Therefore further measurements in this temperature range were conducted for the optimisation. The parameters of the α_{max} model are kept the same, and all the optimised parameters of the model are shown in Table 3, B-stage kinetic model. The fit of the model is shown in the squares in Fig. 7. The fit is

Table 2
Results of dynamic DSC measurements made at heating rates of 10, 5, 2.5, and 1 °C/min, used for the kinetic modelling.

Heating rate (°C/min)	Reaction enthalpy, ΔH_{dyn} (J/g)
1	438
1	438
2.5	457
2.5	443
5	415
5	412
10	425
10	419

Table 3
Parameters of the global and B-stage kinetic model, and the glass transition temperature model.

Name	Symbol	Global kinetic model	B-stage kinetic model
Resin kinetics			
Frequency factor	k_1 (s^{-1})	$4.36553 \cdot 10^{-4}$	$3.9304 \cdot 10^{-4}$
Activation energy	E_1 (–)	17.107	16.615
Reference temperature	T_{ref} (K)	433	433
Reaction exponent	n (–)	0.04	0.04
Polynomial parameter	G_0 (–)	0.1377	0.1293
Polynomial parameter	G_1 (–)	2.9714	2.0098
Polynomial parameter	G_2 (–)	−1.1668	12.928
Polynomial parameter	G_3 (–)	−19.736	−78.495
Polynomial parameter	G_4 (–)	75.072	177.9
Polynomial parameter	G_5 (–)	−105.77	−186.31
Polynomial parameter	G_6 (–)	48.567	71.896
T_g of the uncured resin	T_{g0} (K)	257.5 (°C)	257.5
T_g of the fully cured resin	$T_{g\infty}$ (K)	458	458
Adjustable parameter	μ (–)	0.3	0.3
Glass transition temperature			
T_g of the uncured resin	T_{g0} (°C)	−15.5	−15.5
T_g of the fully cured resin (fitted)	$T_{g\infty}$ (°C)	245	245
	λ (–)	0.5052	0.5052

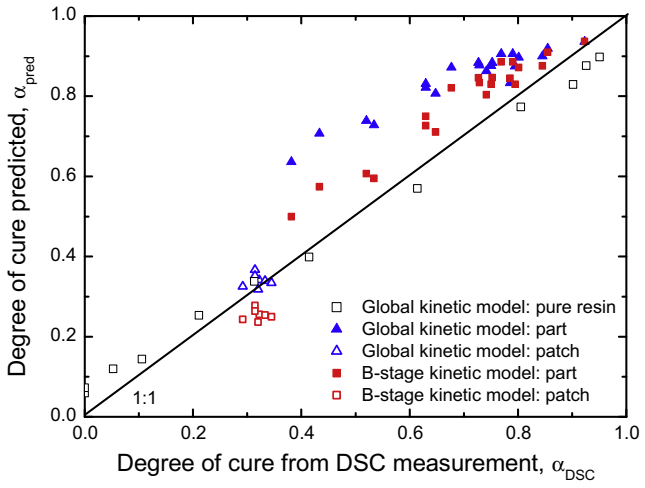

Fig. 7. Modelled values of degree of cure, α, versus those measured using DSC using both the global kinetic model based on isothermal measurements from 120 to 180 °C, and the improved B-stage kinetic model based on isothermal measurements in the range 154–166 °C (based on mould temperature sensor close to cavity in composite processing). (For interpretation of the references to colour in this figure legend, the reader is referred to the web version of this article.)

improved from an R^2 value of 0.69 in the global kinetic model to 0.90 in the B-stage kinetic model.

5.3. Co-curing of the CFRP part and patch

Both CFRP patches and CFRP parts were manufactured using the outlined procedure. A co-cured structural reinforcement was possible with an applied pressure of 2 MPa. An example micrograph of a tested bearing section is shown in Fig. 8. The schematic identifies a section a to b, referring to the composite local reinforcement from the outer most edge of the patch to the bearing surface. The interface between the CFRP part and CFRP patch is indicated by the red dotted line. Optical measurement of the fibre volume content was conducted to study both components before and after B-stage. The fibre volume content of the part was found to remain constant at 63 ± 3%, indicating that resin did not flow out from the part during co-curing. The patch volume fraction was measured as 50 ± 6% before B-stage, and increase to 65 ± 5% as circa 1.5 ml was lost from the patch during the consolidation process. The image in Fig. 8 indicates that a void free bond was possible, with no evidence of porosity in the interface between the part and patch. Damage accumulation in the right side of the image also display evidence of kink bands due to compression stresses which transition into the thin ply laminate architecture patch; serving as further evidence of good interface.

5.4. Discussion

The results demonstrate that B-stage cure profiles may successfully be applied to the studied epoxy resin, where the part may be free standing and the patch is consolidated with local pressure. The progression of α and T_g were successfully described and produced consistent results when compared to measurements using DSC. A single model to describe this processing approach with various degree of partial cures proved to be very powerful to identify ideal processing windows; it was however also observed that a very accurate temperature monitoring is required to reach the required precision. We also note that the principle of introducing excess matrix to the B-stage patch, to provide enough resin for adhesion seems to be a valid approach. Our best results were obtained when working with 30% cured B-stage patches and 75% cured B-stage parts, could be co-cured into low porosity, void free composites and interface.

6. Conclusions

This work demonstrated an approach for using the developed kinetic model to describe the B-stage curing and co-curing assembly of local reinforcement. By prediction and experimental validation, two composites sub-parts with identical matrix were successfully joined with one part having a preceding T_g, and the other one having a T_g lagging in respect to the curing temperature. The described methodology to locally reinforce a partially cured structure has proved to be possible and presents techniques that are readily scalable, and cost effective. Further, the proposed co-curing methodology is free of adhesives. The procedure may therefore be directly applied to aerospace manufacturing without further additional certification. Co-curing of B-stage cured CFRP patches onto B-stage cured CFRP parts has been shown as to be possible from a cure kinetics perspective. The formation of void

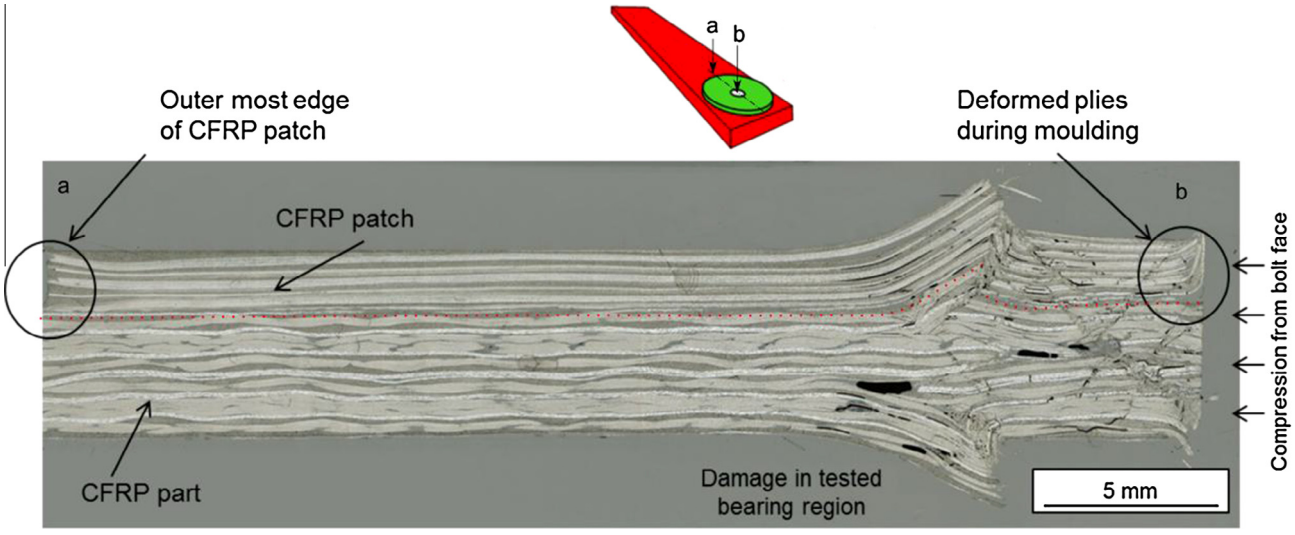

Fig. 8. Optical micrograph of the assembled, co-cured CFRP part to the CFRP patch after a double lap bearing test. Red indicates the interface between the two components. (For interpretation of the references to colour in this figure legend, the reader is referred to the web version of this article.)

free surfaces was also demonstrated. The biggest challenge for industrialisation is to the narrow window for the free standing cure of the CFRP part presented by the RTM6 resin system. Other amine curing epoxies were explored and present far better suitability when free standing co-curing was required. By understanding the cure kinetics and T_g development of a resin system, possible cure cycles were evaluated to fit the prerequisites of the approach. The co-curing of B-stage parts provides very interesting possibilities for joining of structures, especially using combined manufacturing processes (e.g. infusion, prepregs, conventional RTM and/or compression RTM) that could be an extremely cost effective approach for the joining of structures.

Acknowledgements

This work was carried out within the collaborative research project Cost Effective Reinforcement of Fasteners in Aerospace Composites (CERFAC) funded by the European Commission, Grant agreement no. 266026, within the Seventh Framework Programme. The authors also thank the Swiss Competence Centre for Energy Research (SCCER – Capacity Area A3: Minimization of energy demand). A. Keller, F. Leone and S. Ruf, are gratefully acknowledged for their contributions.

References

[1] Administration FA. Advisory circular 20-107B on composite aircraft structure; 2009.
[2] Teoh KJ, Hsiao K-T. Improved dimensional infidelity of curve-shaped VARTM composite laminates using a multi-stage curing technique – experiments and modeling. Compos Part A: Appl Sci Manuf 2011;42(7):762–71.
[3] White SR, Kim YK. Staged curing of composite materials. Compos Part A: Appl Sci Manuf 1996;27(3):219–27.
[4] Griffiths B, Noble N. Process and tooling for low cost, rapid curing of composites structures. SAMPE J 2004;40(1):41–6.
[5] Corbett T et al. Characterization of melded carbon fibre/epoxy laminates. Compos Part A: Appl Sci Manuf 2007;38(8):1860–71.
[6] Bond DN, Nesbitt A; Coenen V, Brosius D. The evaluation and development of the quickstep out-of-autoclave composites processing method. In: Composites processing, Stoke-on-Trent, UK; 2005.
[7] Seferis JC, Tillman MS, Hayes BS. Scaled analysis of composite adhesive interphase properties. J Macromol Sci-Phys 2001;B 40(5):923–34.
[8] Kim K-S et al. Failure mode and strength of uni-directional composite single lap bonded joints with different bonding methods. Compos Struct 2006;72(4):477–85.
[9] Moosburger-Will J et al. Joining of carbon fiber reinforced polymer laminates by a novel partial cross-linking process. J Appl Polym Sci 2015;132(27).
[10] Ersoy N et al. Development of the properties of a carbon fibre reinforced thermosetting composite through cure. Compos Part A: Appl Sci Manuf 2010;41(3):401–9.
[11] Huang CK. Study on co-cured composite panels with blade-shaped stiffeners. Compos Part A: Appl Sci Manuf 2003;34(5):403–10.
[12] Wang X et al. Experimental investigation of the compaction and tensile strength of co-cured skin-to-stiffener structures. Appl Compos Mater 2011;18(5):371–83.
[13] Hsieh TH et al. The toughness of epoxy polymers and fibre composites modified with rubber microparticles and silica nanoparticles. J Mater Sci 2010;45(5):1193–210.
[14] Giannakopoulos I, Masania K, Taylor AC. Toughening of epoxy using core–shell particles. J Mater Sci 2011;46(2):327–38.
[15] Amacher R et al. Thin ply composites: experimental characterization and modeling of size-effects. Compos Sci Technol 2014;101:121–32.
[16] Kamal MR, Sourour S. Kinetics and thermal characterization of thermoset cure. Polym Eng Sci 1973;13(1):59–64.
[17] Barton J. The application of differential scanning calorimetry (DSC) to the study of epoxy resin curing reactions. In: Epoxy resins and composites I. Berlin/Heidelberg: Springer; 1985. p. 111–54.
[18] DiBenedetto AT. Prediction of the glass transition temperature of polymers: a model based on the principle of corresponding states. J Polym Sci, Part B: Polym Phys 1987;25(9):1949–69.
[19] Batch GL, Macosko CW. Kinetic model for crosslinking free radical polymerization including diffusion limitations. J Appl Polym Sci 1992;44(10):1711–29.
[20] Bailleul J-L, Delaunay D, Jarny Y. Determination of temperature variable properties of composite materials: methodology and experimental results. J Reinf Plast Compos 1996;15(5):479–96.
[21] Yousefi A, Lafleur PG, Gauvin R. Kinetic studies of thermoset cure reactions: a review. Polym Compos 1997;18(2):157–68.
[22] Han S et al. Kinetic study of the effect of catalysts on the curing of biphenyl epoxy resin. J Appl Polym Sci 1998;68(7):1125–37.
[23] Ruiz E, Trochu F. Thermomechanical properties during cure of glass-polyester RTM composites: elastic and viscoelastic modeling. J Compos Mater 2005;39(10):881–916.
[24] Ruiz E, Billotte C. Predicting the cure of thermosetting polymers: the isoconversion map. Polym Compos 2009;30(10):1450–7.
[25] Keller A et al. Fast-curing epoxy polymers with silica nanoparticles: properties and rheo-kinetic modelling. J Mater Sci 2016;51(1):236–51.
[26] Moosburger-Will J et al. Influence of partial cross-linking degree on basic physical properties of RTM6 epoxy resin. J Appl Polym Sci 2013.
[27] Hexcel_Corporation. HexFlow RTM6 product data; 2012.
[28] ASTM. Standard test method for bearing response of polymer matrix composite laminates; 2008.
[29] Reading M, Hourston J. Modulated-temperature differential scanning calorimetry: theoretical and practical applications in polymer characterisation. Springer; 2006.
[30] Riesen R. Collected applications thermal analysis thermosets. Schwerzenbach: Mettler Toledo; 2006.
[31] Pascault JP, Williams RJJ. Glass-transition temperature versus conversion relationships for thermosetting polymers. J Polym Sci Part B-Polym Phys 1990;28(1):85–95.
[32] Urbaniak M. A relationship between the glass transition temperature and the conversion degree in the curing reaction of the EPY (R) epoxy system. Polimery 2011;56(3):240–3.
[33] Aduriz XA et al. Quantitative control of RTM6 epoxy resin polymerisation by optical index determination. Compos Sci Technol 2007;67(15–16):3196–201.
[34] Karkanas PI, Partridge IK. Cure modeling and monitoring of epoxy/amine resin systems. II. Network formation and chemoviscosity modeling. J Appl Polym Sci 2000;77(10):2178–88.
[35] Karkanas PI, Partridge IK. Cure modeling and monitoring of epoxy/amine resin systems. I. Cure kinetics modeling. J Appl Polym Sci 2000;77(7):1419–31.
[36] Abou Msallem Y et al. Material characterization and residual stresses simulation during the manufacturing process of epoxy matrix composites. Compos Part A: Appl Sci Manuf 2010;41(1):108–15.
[37] Prulière E et al. An efficient reduced simulation of residual stresses in composite forming processes. Int J Mater Form 2010;3(2):1339–50.
[38] Lange J et al. Understanding vitrification during cure of epoxy resins using dynamic scanning calorimetry and rheological techniques. Polymer 2000;41(15):5949–55.